Extraordinary terahertz transmission through subwavelength spindle-like apertures in NbN film*

Zheng Xiao-Rui(郑小睿)[a)†], Cheng Fei(程 飞)[a)], Wu Jing-Bo(吴敬波)[b)], Jin Biao-Bing(金飚兵)[b)], and Zhu Bei-Yi(朱北沂)[a)]

[a)] National Laboratory for Superconductivity, Institute of Physics and Beijing National Laboratory for Condensed Matter Physics, Chinese Academy of Sciences, Beijing 100190, China

[b)] Research Institute of Superconductor Electronics (RISE), School of Electronic Science and Engineering, Nanjing University, Nanjing 210093, China

(Received 10 May 2013; revised manuscript received 10 July 2013; published 19 November 2013)

We studied numerically the temperature dependent extraordinary terahertz transmission through niobium nitride (NbN) film perforated with subwavelength spindle-like apertures. Both the resonant frequency and intensity of extraordinary terahertz transmission peaks can be greatly modified by the transition of NbN film from the normal state to the superconducting state. An enhancement of the $(\pm 1,0)$ NbN/magnesium oxide (MgO) peak intensity as high as 200% is demonstrated due to the combined contribution of both the superconducting transition and the excitation of localized surface plasmons (LSPs) around the apertures. The extraordinary terahertz transmission through spindle-like hole arrays patterned on the NbN film can pave the way for us to explore novel active tuning devices.

Keywords: extraordinary terahertz transmission, superconducting transition, spindle-like apertures, localized surface plasmon mode

PACS: 41.20.Jb, 73.20.Mf **DOI:** 10.1088/1674-1056/23/1/014101

1. Introduction

The discovery of extraordinary optical transmission (EOT) has attracted enormous interest due to its underlying physical mechanism as well as potential engineering applications.[1–5] Surface plasmon polaritons (SPPs) are generally believed to assist the EOT.[6] The frequency and intensity of the EOT peaks depend on how SPPs are excited and propagate, which are determined by the geometry of the structures, as well as the intrinsic properties of the metal and surrounding dielectrics.[7] The dependence of EOT spectra on the materials were studied extensively[8–10]; superconducting films show a greater enhancement and tuning ability on resonant behaviors compared to noble metals.[11–14] For low-temperature superconducting film, such as Nb and NbN, have lower real conductivities and thus lower absorptions, from which the propagation of SPPs will benefit a great deal.[3,11]

On the other hand, the localized surface plasmons (LSPs) associated with the hole shape also play an important role in the EOT.[15] Optical properties of different types of apertures have been studied from the visible to terahertz (THz) regime during the last few years.[16–20] A special type of aperture with a bow-tie shape has been investigated to improve the transmission efficiency recently.[21–25] The intense interaction between two closely spaced triangular slots leads to a strong electric field distribution and localization compared to those of square and rectangular apertures with the same filling fraction. In this paper, extraordinary terahertz transmission of NbN film perforated with spindle-like hole arrays has been studied numerically. The effects of SPPs or LSPs on the transmittance and shift of resonance frequency have been discussed. Our results demonstrate that spindle-like hole arrays patterned on superconducting film provide a more flexible way to actively control the resonant frequency and amplitude of extraordinary terahertz transmission.

2. Simulation setup

Our simulations were carried out using the finite-difference time domain (FDTD) method. The 200-nm-thick NbN films were designed on 500-μm-thick MgO substrates. A set of spindle-like hole arrays were patterned on the NbN film with different geometrical parameters, as shown in Fig. 1. Each NbN sample is composed of periodic spindle-like apertures with a fixed arm length, width and tip-to-tip gaps of 100 μm, 25 μm and 2 μm, respectively, with various tip lengths ranging from 0 to 50 μm. The spacing in the x and y directions are 100 μm and 102 μm, respectively. The polarization of the incident light is along the x axis so that the oscillation of LSPs around the hole edge is the strongest among all possible input orientations.[26] The transmission spectra of NbN samples were calculated in a temperature range of 8.2 K–300 K. The temperature dependent complex permittivity of NbN is calculated based on the framework of BCS theory.[27]

*Project supported by the National Basic Research Program of China (Grant Nos. 2011CBA00110 and 2011CBA00107) and the National Natural Science Foundation of China.

†Corresponding author. E-mail: zhengxiaorui1986@hotmail.com

© 2014 Chinese Physical Society and IOP Publishing Ltd

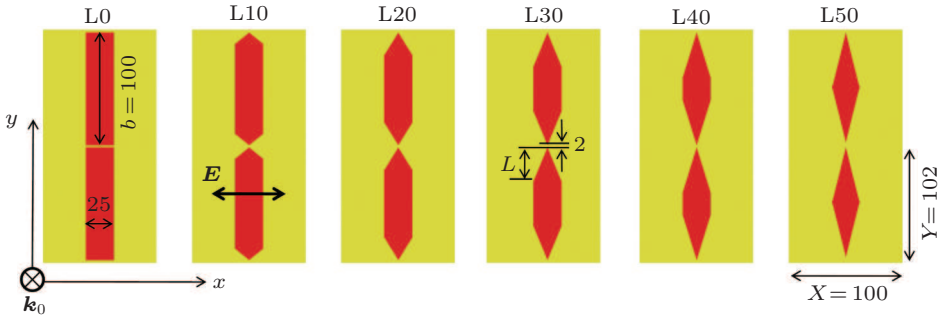


Fig. 1. (color online) Schematic diagram of spindle-like unit cells. The tip lengths (L) of the six samples (L0, L10, L20, L30, L40 and L50) are 0, 10 μm, 20 μm, 30 μm, 40 μm and 50 μm, respectively. The polarization of the incident light is along the x axis. All dimensions are in micrometres.

3. Effect of superconducting transition on EOT

The zero-order transmission spectra of L0 from 8.2 K to 300 K are shown in Fig. 2. The transmission peaks can be indexed according to momentum matching conditions of SPPs, which can be expressed as follows:[2]

$$\boldsymbol{k}_{\rm sp} = \boldsymbol{k}_0 \cdot \sin\theta \pm n\boldsymbol{G}_x \pm m\boldsymbol{G}_y. \tag{1}$$

The n and m are integers, $\boldsymbol{G}_x$ and $\boldsymbol{G}_y$ are the reciprocal lattice vectors, $\boldsymbol{k}_0$ is the wave vector of the incident light and θ is the incident angle. For normal incidence ($\theta = 0$) and TM polarization in our case, the resonance around 0.6 THz corresponds to the $(\pm1,0)$ modes excited on the interface between NbN film and MgO substrate. The transmission spectrum experiences remarkable changes as the temperature decreases from 300 K to 8.2 K. Specifically, the spectrum remains unchanged when the temperature is above the typical critical temperature of NbN film ($T_{\rm c} = 15.8$ K). With a further reduction of temperature, the magnitude of $(\pm1,0)$ NbN/MgO peak increases dramatically from 0.33 at 18 K to 0.74 at 8.2 K, indicating a 124% enhancement with the transition of NbN film from the normal state to the superconducting state. The resonant frequency, on the other hand, decreases from 0.61 THz at 18 K to 0.50 THz at 8.2 K.

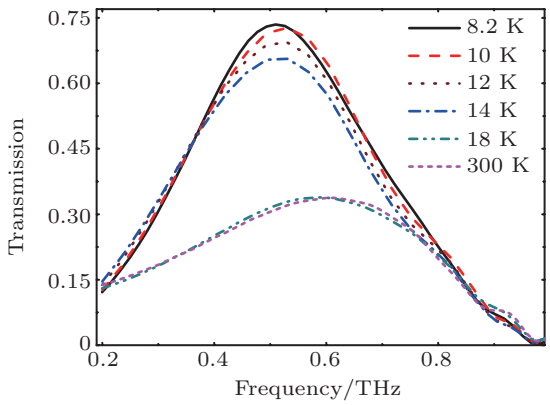


Fig. 2. (color online) Zero-order transmission spectra of L0 at various temperatures.

To understand the dependence of the spectrum on the temperature, we examined here the temperature dependent permittivity of NbN film. Figure 3(a) shows the complex permittivity of NbN film ($\varepsilon_m = \varepsilon_1 + {\rm i}\varepsilon_2$) at 0.6 THz as a function of temperature. The real part of permittivity ε_1 is negative, which indicates a metallic response; its magnitude increases dramatically once the NbN film goes into the superconducting state. The imaginary part of permittivity ε_2 decreases obviously below $T_{\rm c}$, indicating a weaker internal damping of NbN film for SPPs.[3] To further evaluate the loss mechanism, in Fig. 3(b) we calculated the propagation length $\delta_{\rm sp}$ of SPPs, which can be expressed as

$$\delta_{\rm sp} = \frac{1}{2{\rm Im}(\boldsymbol{k}_{\rm sp})} = \lambda_0 \frac{{\varepsilon_1}^2}{2\pi\varepsilon_2}\left(\frac{\varepsilon_1+\varepsilon_{\rm d}}{\varepsilon_1\varepsilon_{\rm d}}\right)^{3/2}, \tag{2}$$

where $\varepsilon_{\rm d}$ is the permittivity of the substrate ($\varepsilon_{\rm d} = 9.4$ for our MgO substrate), $\boldsymbol{k}_{\rm sp}$ is the wave vector of SPPs and λ_0 is the wavelength in free space, respectively. The theoretical $\delta_{\rm sp}$ calculated from Eq. (2) is found to increase from 0.099 m at 300 K to 6.3 m at 8.2 K as NbN film transits from the normal state to the supercuducting state. Therefore, the enhancement of transmittance is attributed to the smaller amount of internal damping of NbN film and hence the prolonged propagation distance of SPPs in the superconducting state than that in the normal state.[11]

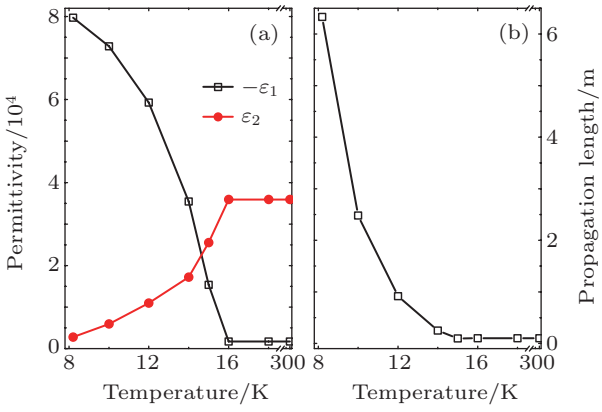


Fig. 3. (color online) Temperature dependent permittivity of NbN film (a) and propagation length of SPPs (b) at 0.6 THz.

On the other hand, the redshift of peak frequency is ascribed to the change of ε_1. According to the dispersion relationship of SPPs, the peak position is determined by the real

part of $\boldsymbol{k}_{\rm sp}$

$$\mathrm{Re}(\boldsymbol{k}_{\rm sp}) = k_0\left(\frac{\varepsilon_1\varepsilon_{\rm d}}{\varepsilon_1+\varepsilon_{\rm d}}\right)^{1/2}, \tag{3}$$

plotted as the dash lines in Fig. 4(b). As ε_1 decreases, $\mathrm{Re}(\boldsymbol{k}_{\rm sp})$ is found to decrease as the NbN film goes into the superconducting state, which results in a redshift of 0.1 THz of $(\pm1,0)$ NbN/MgO modes.

4. Transition from SPP to LSP mode by geometrical modulation

To investigate the effect of geometric modulation on the extraordinary terahertz transmission through spindle-like hole arrays, we have examined the zero-order transmission spectra of the L50 under different temperatures, as shown in Fig. 4(a), where $(\pm1,0)$ NbN/MgO modes are found at around 0.7 THz. The temperature dependent spectrum shows a similar behaviour to that of L0 as the transition from the normal state to the superconducting state of NbN film. The peak intensity increases dramatically from 0.24 at 18 K to 0.72 at 8.2 K, i.e., a 200% enhancement, which is larger than the 124% enhancement of L0. The greater enhancement results from both the smaller amount of internal damping of SPPs in the superconducting relative to the normal state and the stronger electric field distributions around the spindle-like apertures in L50. The peak frequency, decreasing from 0.74 THz at 18 K to 0.72 THz at 8.2 K, is insensitive to the permittivity change of NbN film and has less redshift than L0. The dependence of resonant frequency of L50 on the incident angle at 8.5 K is examined in Fig. 4(b), accompanied by the theoretical dispersion relation of $(\pm1,0)$ NbN/MgO modes as a reference. The degenerate $(\pm1,0)$ NbN/MgO modes split into two new bands indicating

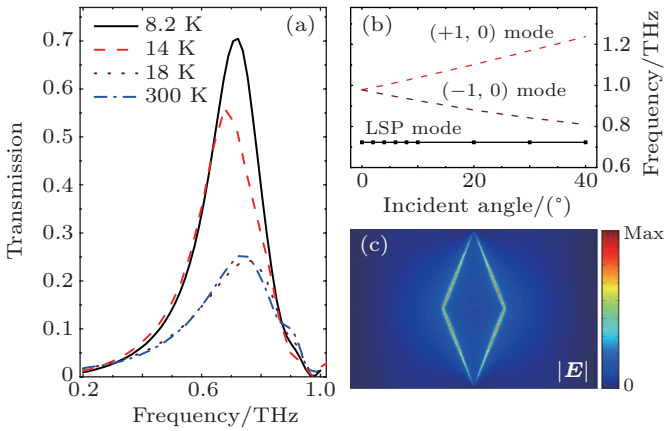


Fig. 4. (color online) (a) Zero-order transmission spectra of L50 at various temperatures under TM polarization. (b) The dispersion relations of both LSPs and $(\pm1,0)$ NbN/MgO modes. (c) The electric field distributions ($|\boldsymbol{E}|$) for L50 at 0.75 THz evaluated at 1 nm below the interface in the MgO substrate.

the propagation nature of this mode. The LSP mode, however, remains unchanged with the incident angle, which implies that the LSP mode dominates the EOT of L50, shown as the black curve in Fig. 4(b).

To further understand the effect of the localized surface plasmon mode around spindle-like apertures on the peak intensity and resonant frequency, the normalized transmission spectra of a set of spindle-like patterns at 8.2 K are shown in Fig. 5(a). The transmission intensity was normalized to the area occupied by the hole arrays. The dependence of both peak intensity and frequency on L are plotted in Fig. 5(b). The $(\pm1,0)$ NbN/MgO modes are found to blueshift as the tip length is lengthened, which increase from 0.51 THz for $L = 0$ to 0.72 THz for $L = 30$ μm. With a further increase of L from 30 μm to 50 μm, however, the peak frequency remains almost the same. The blueshift results from LSPs of different spindle-like apertures, which behaves as an individual rectangular waveguide with the cutoff wavelength $\lambda_{\rm c} = 2b$, where b is the longer edge of the rectangle. As L increases from 0 to 30 μm, the effective length of the rectangular aperture decreases and the cutoff wavelength is reduced accordingly, which causes the blueshift of the transmission peaks. As L further increases from 30 μm to 50 μm, a negligible shift of the peak frequency was observed, due to the smaller variation of the effective length of the spindle-like apertures. Meanwhile, the normalized transmission increases with L and can reach as large as 5.75 for the case of $L = 50$ μm. With the periodicity and temperature unchanged, hence the same propagation length of SPPs, an additional enhancement of intensity comes from the stronger electric field enhancement distributed at the hole edge of spindle-like apertures, as shown in Fig. 4(c). To further evaluate the enhancement effect induced by the LSP mode around the spindle-like structures, the dependence of peak intensity enhancement of the superconducting state (8.2 K) relative to the normal state (300 K) on L is shown in Fig. 5(c). We note that the enhancement factor is boosted as L increases from 0 to 50 μm, following approximately a linear relationship. In this way, the proposed spindle-like hole arrays are shown to benefit a great deal the extraordinary terahertz transmission through the superconducting film.

The resonance frequency ($f_{\rm r}$) of subwavelength structures made on superconducting films is, on one hand, determined by their estimated or effective geometrical parameters, demonstrated in Fig. 5; on the other hand, the low Ohmic loss resonances at the superconducting state rely on the superconductor itself. For example, due to the limitation of gap frequency ($f_{\rm g} = 2\Delta_0/h$, where Δ_0 is the energy gap at 0 K and h is the Planck constant), the THz metamaterials (MMs) made from Nb films can only obtain low loss resonances below 0.7 THz.[28] For NbN films with a higher gap frequency ($f_{\rm g} = 1.18$ THz), a relatively wide (30%) tuning range of

MMs with f_r approaching f_g was observed due to a significant change of the kinetic inductance of the superconducting film, which can be further increased by decreasing the film thickness.[29] However, as the frequency of incident photons is larger than f_g, almost all paired electrons at a superconducting state are broken into quasi-particles, leading to the abrupt increase of surface resistance and thus a degenerate resonant performance of superconducting structures. In this way, a resonance frequency slightly less than f_g is preferable when we utilize superconducting materials, such as NbN films, to acquire a low Ohmic loss and large tuning range.

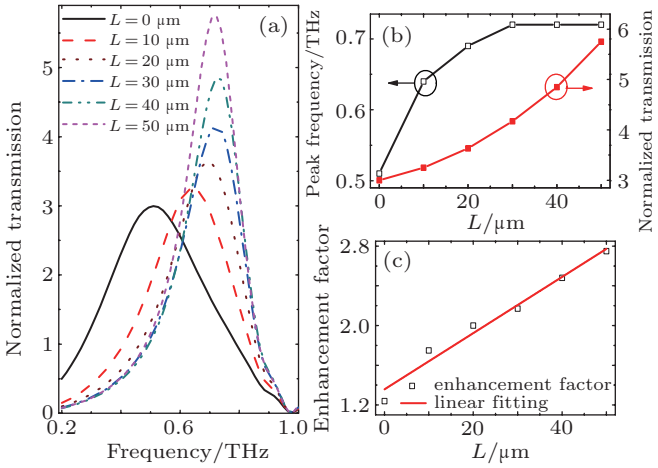


Fig. 5. (color online) (a) Normalized transmission spectrum of a set of spindle-like patterns at 8.2 K. (b) The dependence of peak frequency and normalized transmission on L. (c) The dependence of peak intensity enhancement of the superconducting state relative to the normal state on L.

5. Conclusions

In conclusion, the extraordinary terahertz transmission of NbN film perforated with spindle-like hole arrays has been studied numerically. Both the peak intensity and resonant frequency of $(\pm 1, 0)$ NbN/MgO modes experience a dramatic change with the transition of NbN film from the normal state to the superconducting state, which is attributed to the temperature-dependent permittivity of NbN film. Moreover, the spindle-like apertures boost an enhancement of $(\pm 1, 0)$ NbN/MgO peak intensity as high as 200% due to the combined contribution of both the superconducting transition and the excitation of LSPs around the apertures. We propose that the spindle-like structures patterned on the NbN film may serve as a promising platform of novel active tuning devices, such as modulators, filters, sensors and so on.

References

[1] Ebbesen T W, Lezec H J, Ghaemi H F, Thio T and Wolff P A 1998 *Nature* **391** 667
[2] Barnes W L, Dereux A and Ebbesen T W 2003 *Nature* **424** 824
[3] Genet C and Ebbesen T W 2007 *Nature* **445** 39
[4] Gordon R, Hughes M, Leathem B, Kavanagh K L and Brolo A G 2005 *Nano Lett.* **5** 1243
[5] Cheng F, Liu H F, Li B H, Han J, Xiao H, Han X F, Gu C Z and Qiu X G 2012 *Appl. Phys. Lett.* **100** 131110
[6] Ghaemi H F, Thio T, Grupp D E, Ebbesen T W and Lezec H J 1998 *Phys. Rev. B* **58** 6779
[7] Garcia-Vidal F J, Martin-Moreno L, Ebbesen T W and Kuipers L 2010 *Rev. Mod. Phys.* **82** 729
[8] Grupp D E, Lezec H J, Ebbesen T W, Pellerin K M and Thio T 2000 *Appl. Phys. Lett.* **77** 1569
[9] Rodrigo S G, Garcia-Vidal F J and Martin-Moreno L 2008 *Phys. Rev. B* **77** 075401
[10] Cheng F, Li B H, Han J, Xiao H, Gu C Z and Qiu X G 2013 *Appl. Phys. Lett.* **102** 151113
[11] Wu J B, Dai H, Wang H, Jin B B, Jia T, Zhang C H, Cao C H, Chen J, Kang L, Xu W W and Wu P H 2011 *Opt. Express* **19** 1101
[12] Fang X, Zhuang C G, Wen Z C, Han X F, Feng Q R, Xi X X, Nori F, Xie X C, Niu Q and Qiu X G 2011 *Phys. Rev. B* **84** 205438
[13] Tian Z, Singh R, Han J G, Gu J Q, Xing Q R, Wu J and Zhang W L 2010 *Opt. Lett.* **35** 3586
[14] Tsiatmas A, Buckingham A R, Fedotov V A, Wang S, Chen Y, de Groot P A J and Zheludev N I 2010 *Appl. Phys. Lett.* **97** 111106
[15] Klein Koerkamp K J, Enoch S, Segerink F B, van Hulst N F and Kuipers L 2004 *Phys. Rev. Lett.* **92** 183901
[16] Fan W J, Zhang S, Malloy K J and Brueck S R J 2005 *Opt. Express* **13** 4406
[17] Lu X C, Han J G and Zhang W L 2008 *Appl. Phys. Lett.* **92** 121103
[18] Zhang W L 2008 *Eur. Phys. J. Appl. Phys.* **43** 1
[19] Azad A K and Zhang W L 2005 *Opt. Lett.* **30** 2945
[20] Beruete M, Sorolla M, Campillo I and Dolado J S 2005 *IEEE Microwave Wireless Compon. Lett.* **15** 116
[21] Kato E, Suizu K and Kawase K 2009 *Appl. Phys. Express* **2** 122302
[22] Wang L, Uppuluri S M, Jin E X and Xu X F 2006 *Nano Lett.* **6** 361
[23] Kinzel E C and Xu X 2010 *Opt. Lett.* **35** 992
[24] Wang L and Xu X F 2007 *Appl. Phys. Lett.* **90** 261105
[25] Yang Y P, Singh R and Zhang W L 2011 *Opt. Lett.* **36** 2901
[26] Degiron A, Lezec H J, Yamamoto N and Ebbesen T W 2004 *Opt. Commun.* **239** 61
[27] Kang L, Jin B B, Liu X Y, Jia X Q, Chen J, Ji Z M, Xu W W, Wu P H, Mi S B, Pimenov A, Wu Y J and Wang B G 2011 *J. Appl. Phys.* **109** 033908
[28] Zhang C H, Wu J B, Jin B B, Ji Z M, Kang L, Xu W W, Chen J, Tonouchi M and Wu P H 2012 *Opt. Express* **20** 42
[29] Wu J B, Jin B B, Xue Y H, Zhang C H, Dai H, Zhang L B, Cao C H, Kang L, Xu W W, Chen J and Wu P H 2011 *Opt. Express* **19** 12021